Mixed-phase boundary layer clouds terminate the ozone depletion events in the Arctic region

Xiao-Ming Hu, Fuqing Zhang, Guo Yu, and Jose D Fuentes

Department of Meteorology, Pennsylvania State University, University Park, Pennsylvania

Longtao Wu

Jet Propulsion Laboratory, California Institute of Technology, Pasadena, California

July 11, 2011

To be Submitted to *GRL*

Corresponding author address: Dr. Xiao-Ming Hu, Department of Meteorology, The Pennsylvania State University, University Park, PA 16802.

Email: xzh3@psu.edu

Abstract

Ozone depletion events (ODEs) are frequently observed near the surface in the Arctic area in spring. While their formation mechanism seems to be understood, their termination mechanisms remain unclear. Gong et al. (1997) and Strong et al. (2002) reported that wind shear above the boundary layer could induce enough vertical mixing to transport O_3-richer air from aloft to replenish surface O_3, thus terminate the ODEs. Jacobi et al. (2010) illustrated that O_3-richer air mass from midlatitudes moving northward into the Arctic may terminate the ODEs. In this study a new mechanism related to mixed-phase boundary layer clouds is proposed. A single layer stratocumulus deck observed over Barrow, Alaska (AK) on April 8, 2008 is simulated using high-resolution (in both horizontal and vertical directions) WRF/Chem model. The effect of such mixed-phase boundary layer clouds to the ODEs is simulated by including a tracer in the simulation. The initial profile of the tracer is set as the O_3 profile during a typical ODE. It is found that the cloud-top radiative cooling can induce strong downdrafts and updrafts. The downdrafts due to the mixed-phase boundary layer cloud can bring O_3-richer air from above downward to terminate the ODE.

1. Introduction

Anomalously low ozone (O_3) mixing ratios in the atmospheric boundary layer (ABL) during spring in the Arctic area were reported since 1980s (Oltmans, 1981; Bottenheim et al., 1986; Barrie et al., 1988). Such yearly O_3 depletion events (ODEs) in the Arctic area attracted extensive research since then (Mickle et al., 1989; Oltmans et al., 1989; Anlauf et al., 1994;

Leaitch et al., 1994; Solberg et al., 1996; Rasmussen et al., 1997; Hopper and Hart, 1994; Hopper et al., 1998; Sumner and Shepson, 1999; Bottenheim et al., 2002; 2009; Tarasick and Bottenheim, 2002; Bottenheim and Chan, 2006, Jacobi et al., 2006; Helmig et al., 2007; Eneroth et al., 2007; Jacobi et al., 2010). It is now generally accepted that the halogen (especially bromine) activation and the subsequent reactions caused onset of the ODEs (Barrie et al., 1988; Fan and Jacob, 1992; Boudries and Bottenheim, 2000; Rankin et al., 2002; Simpson et al., 2007; Grannas et al., 2007; Piot and von Glasow, 2008; Hara et al., 2010; Frieß et al., 2011). While the basic features of the ODEs seem understood, several questions remain unclear (Bottenheim et al., 2002; Jacobi et al., 2006; 2010). First, why are the ODEs only observed in spring, but not other seasons? (Bottenheim et al., 2002; Lehrer et al., 2004). Second, what is the spatial extent of the ODEs? (Jacobi et al., 2006; 2010). Third, what are the processes that cause the termination of the ODEs, transport (vertical or horizontal?) or chemical reactions? (Gong et al., 1997; Hopper et al., 1998; Strong et al., 2002; Bottenheim et al., 2009; Jacobi et al., 2010). This paper focuses on the third question.

Previous studies (e.g., Gong et al., 1997; Strong et al., 2002) indicated that wind shear just above the Arctic ABL can contribute to the transport of O_3-richer air from aloft to the surface, thus terminate the ODEs. Jacobi et al. (2010) reported that northward moving lows may bring O_3-rich air from midlatitudes to the Arctic, leading to the termination of the ODEs. In this study, we will provide another mechanism for the termination of the ODEs. We investigated the ODEs in Barrow, AK in spring of 2009 (during which the field campaign of Ocean-Atmosphere-Sea Ice-Snowpack Interactions in Polar Regions (OASIS) 2009 was conducted). During the recovery periods of some ODEs (e.g., March 16, 2009), surface wind speeds kept calm, wind shear in the boundary layer kept low and air mass kept come from the Arctic basin. Thus horizontal transport was less likely the reason for the termination of the ODEs and vertical mixing was unlikely induced solely by wind shear as the cases reported in Strong et al. (2002). For the case of March 16, 2009 boundary layer clouds were noticed in presence during the recovery period. The Arctic boundary layer clouds could strongly impact the vertical structure of the boundary layer through cloud-top radiative cooling and generation of negative buoyancy (Pinto, 1998; Morrison and Pinto, 2006). Thus we speculate the Arctic boundary layer cloud is responsible for the termination of the ODEs in some cases.

The role of the Arctic boundary layer cloud in the ODEs is investigated in this study using nested high-resolution three-dimensional model simulation.

2. Model setup and experimental design

The Arctic boundary layer cloud presents challenges to modelers because its unique types and characteristics that are less common at lower latitudes. Previous numerical modeling studies of boundary layer stratocumulus have indicated considerable spread in model solutions (Klein et al., 2009; Morrison et al., 2011). To successfully simulate Arctic boundary layer clouds, a realistic treatment of ice microphysics and proper model resolution are critical (Klein et al., 2009). In this study, a single layer stratocumulus deck observed over the North Slope of Alaska on April 8, 2008 is simulated using the Weather Research and Forecasting model with Chemistry (WRF/Chem) version 3.2.1 (Grell et al. 2005). Most model configurations follow those used in Solomon et al. (2011), in which the same cloud case appears to be successfully simulated. We describe here only the configurations different from those in Solomon et al. (2011) and those that are essential for the simulation of O_3. Three model domains with horizontal grid spacings of 25 km, 5 km, and 1 km used in this study are the same as the first three nested domains used in

Solomon et al. (2011). We do not nest even finer resolution domains since the simulation in the 1 km resolution domain appeares to capture the characteristics of the Arctic mixed-phase cloud (Solomon et al., 2009; 2011). 85 pressure levels below 800 hPa are adopted as Solomon et al. (2011) to better resolve the mixing and entrainment in the mixed-layer and entrainment zone. The National Centers for Environmental Prediction (NCEP) global forecast system (GFS) final (FNL) operational global analyses are used for the initial conditions and boundary conditions of all meteorological variables. The model is spun-up by 12 hours. The simulation starting from 12 UTC, April 8 is used in the analysis. Since the O_3 change rate due to chemical reactions in the Arctic is much slower than that due to transport (Gong et al., 1997), O_3 is represented by a tracer in WRF/Chem to investigate its transport in the presence of boundary layer stratocumulus. The initial and boundary conditions for O_3 is set using a profile of O_3 during a typical ODE, in which O_3 is almost depleted in the lower 300 m near the surface while it is around 45 ppbv in the free troposphere above (Jacobi et al., 2010).

3. Results

In Figure 1, the simulated environmental conditions at Barrow, AK at 18 UTC is compared with the nearest-in-time sounding taken at Barrow at 17.6 UTC, April 8. A well-mixed boundary layer is reproduced by the simulation. However, the simulated boundary layer is slightly lower than the observed by around 100 m. The simulation also captures the temperature and humidity inversion at the top of the boundary layer. Such meteorological conditions are consistent with typical conditions for an Arctic cloud-topped mixed layer (Curry et al., 2000). The humidity and temperature inversion above the cloud-topped mixed layer contributed to the persistence of the cloud deck by inhibiting evaporation associated with entrainment mixing at the cloud top (Curry et al., 2000). Such humidity inversion is a unique feature for Arctic boundary layer clouds. The simulated wind profile is qualitatively similar as the observation: strong shear in the surface layer and at cloud top, weak winds within the cloud and sub-cloud layer.

The simulated spatial distributions of condensed water path in Figure 2 imply simulated cloud passed Barrow after 12 UTC. After the cloud moving to Barrow, the simulated surface O_3 increased by around 15 ppbv from 12 to 16 UTC. By 23 UTC, the surface O_3 increased to 28 ppbv. Thus it appears the presence of cloud plays an important role in replenishing boundary layer O_3 and terminating the ODE.

The vertical structure of cloud ice content, vertical velocity and O_3 are shown in Figure 3. A single layer stratocumulus cloud is successfully simulated in the boundary layer. Liquid water resides at the cloud top, which varies between 1.15 km and 0.9 km along the west-east cross section through Barrow (Figure not shown). The cloud top is at the base of the temperature inversion with a cloud top temperature ranging from -17 to -13^{o}C at Barrow. Cloud ice forms within the liquid cloud layer. Thus the cloud is in mixed phase. Cloud liquid water path dominates cloud ice water path. Total column integrated liquid water accounts for more than 90% of total cloud water (liquid plus ice). The model simulates the mixed-phase stratocumulus starting at 11 UTC with a cloud top at 1.2 km at Barrow. The cloud top slowly descends since then, which is consistent with observation (figure not shown). Strong infrared cooling occurs at the cloud top. Because solar heating is very low due to low sun angle in the Arctic, the cloud shows net cooling (Curry, 1986). The strong infrared cooling near the liquid cloud top generates enough turbulence to promote downdrafts and compensating updrafts (Figure 3b). Cloud top radiative cooling was shown to dominantly trigger the turbulence structure of Arctic boundary layer stratus clouds (Finger and Wendling, 1990). Such radiative-cooling triggered downdrafts are strong enough to reach the surface, which is consistent with the previous studies (e.g., Curry, 1986; Wang et al., 2001; and Zuidema et al., 2005). Before the cloud moves to Barrow, there is a strong temperature inversion near the surface at Barrow. The inversion disappears after the cloud moves in due to that the downdrafts bring warmer air in the upper boundary layer to the surface (Figure not shown). Thus a cloud-top-cooled mixed-layer that extends from the cloud top to the surface forms. Different from a surface-heated convective boundary layer, where downdraft is much weaker than the updraft, the compensating updrafts have about the same strength (~0.6 m s^{-1}) as the downdrafts in this Arctic stratocumulus case (Figure 3b). The comparable size and strength of downdrafts and updrafts is consistent with the observed single-layer, low-level mixed-phase stratiform clouds at Barrow in 2004 (Shupe et al., 2008). The simulated composite structure is consistent with that of an idealized stratus-topped boundary layer reported in Moeng and Schumann (1991), in which the turbulence is maintained solely by cloud-top radiative cooling. It is also consistent with that of a mixed-phase stratus topped boundary layer reported in Morrison and Pinto (2006). Resolved downdrafts and updrafts (Figure 3b) are highly correlated with the vertical distribution of cloud ice (Figure 3a). In the updrafts more cloud ice forms while in the downdraft cloud ice is reduced due to sublimation.

In addition to modifying the boundary layer structure, the downdrafts and updrafts significantly modify the vertical structure of atmospheric constitutes. Since the chemical life time of O_3 is much longer than the time scale of vertical mixing due to downdrafts and updrafts, its vertical distribution is dominated by the transport due to downdrafts and updrafts. The initial O_3 profile is set to an observed profile during a typical ODE, in which O_3 has higher mixing ratios above 300 m than the ozone-depleted boundary layer. The vertical mixing due to downdrafts and updrafts extends to 0.9-1.1 km. Thus the downdrafts could bring O_3-richer air in the upper layers downward to replenish O_3 near the surface. The vertical O_3 profiles at Barrow during the ODEs and in the presence of cloud are shown in Figure 4. The O_3 near the surface is replenished to around 28 ppbv at 23 UTC. This mechanism for the termination of an ODE is consistent with the one-dimensional model simulation reported in Piot and Glasow (2008). However in Piot and Glasow (2008), the details of the phases and dynamics of clouds are not reported. The detailed description of the cloud presence and its interaction with vertical O_3 transport reported in this paper was greatly needed to confirm this ODE termination mechanism (Piot and Glasow, 2008).

4. Conclusions and discussion

Ozone Depletion Events (ODEs) occur regularly in the Arctic boundary layers in spring. This paper illustrates that the mixed-phase clouds commonly occurring in the Arctic area may play important roles in the termination of the ODEs. The mixed-phase cloud can significantly impact the structure of the boundary layer through the influence of cloud-top radiative cooling. Downdrafts and the compensating updrafts induced by the cloud-top radiative cooling can be strong enough to reach the surface. The averaged vertical velocity in the presence of cloud may be as large as 0.6 m s^{-1} in the mixing layer. The vertical mixing due to such updrafts and downdrafts triggered by the clouds can mix the free tropospheric O_3-richer air downward to replenish the O_3 near the surface, thus terminate an ODE.

Note that not all the downdrafts of mixed-phase clouds could reach the surface. The vertical extent of cloud induced mixing depends on cloud top radiative cooling and cloud-base stabilization (Komurcu, 2011). Cloud top radiative cooling of the Arctic mixed-phase cloud is dominated by liquid water (Pinto, 1998). A few factors (e.g., ice nuclei concentration, ice formation mechanism, and crystal habits) could affect clouds liquid water content (Avramov and Harrington, 2010; Komurcu, 2011). Cloud-base stabilization is modulated by the degree of the ice growth and precipitation (Harrington and Olsson, 2001). Whether a mixed-phase cloud could generate strong enough downdrafts to terminate an ODE near the surface depends on complex cloud microphysics and dynamic processes. The sensitivity of strength of cloud circulation (downdrafts and updrafts) is investigated in Komurcu (2011).

The turbulent mixing in the boundary layer due to cloud top radiative cooling has been discovered for many years (Pinto, 1998), however its implication for Arctic O_3 is not widely realized yet. This study may serve as a bridge between the Arctic cloud community and Arctic chemistry community. The new mechanism for the termination of ODEs reported in this study may have profound implication for the spring time Arctic ODEs because of the frequent occurrence of the Arctic mixed-phased clouds. Observations revealed that the Arctic region is cloudy about 85% of the year and mixed-phase clouds dominate low-level clouds within the Arctic during the colder three-quarters of the year (Intrieri et al., 2002; Verlinde et al., 2007). This study also emphasizes that it is necessary for models to adequately simulate mixed-phase boundary layer clouds to reproduce the Arctic ODEs.

The Arctic clouds occurred more frequently and have wider coverage in summer and fall than in spring (Finger and Wendling, 1990; Interieri et al., 2002). A monthly averaged cloud occurrence could be as high as 95% in summer and fall (Interieri et al., 2002). Thus the clouds may enhance vertical mixing through cloud-top radiative cooling more frequently during summer and fall. Such enhancement of vertical mixing in the boundary layer can breakdown the strong surface temperature inversion, which is thought to be one of the prerequisites for ODEs (Lehrer et al., 2004; Bottenheim et al., 2009). Thus higher frequent occurrence and wider coverage of clouds in summer and fall might be linked to the absence of ODEs in those months. Further investigation is greatly needed to confirm such linkage.

Acknowledgement. Guo Yu was supported by the Office of Biological and Environmental Research of the U.S. Department of Energy Grant No. DE-FG02-05ER64058 as part of the Atmospheric System Research Program.

References

Anlauf, K.G., R. E. Mickle, and N. B. A. Trivett (1994), Measurement of ozone during Polar Sunrise Experiment 1992, *J. Geophys. Res.*, 99D(12), 25345–25354.

Avramov, A., and J. Y. Harrington (2010), Influence of parameterized ice habit on simulated mixed phase Arctic clouds, *J. Geophys. Res.*, 115, D03205, doi:10.1029/2009JD012108.

Barrie, L. A., J. W. Bottenheim, R. C. Schnell, P. J. Crutzen, and R. A. Rasmussen (1988), Ozone destruction and photochemical reactions at polar sunrise in the lower Arctic atmosphere, *Nature*, 334, 138–141.

Bottenheim, J. W., A. G. Gallant, and K. A. Brice (1986), Measurements of NO_Y species and O_3 at 82° N latitude, *Geophys. Res. Lett.*, 13(2), 113–116.

Bottenheim, J. W., J. D. Fuentes, D. W. Tarasick, and K. G. Anlauf (2002), Ozone in the Arctic lower troposphere during winter and spring 2000 (ALERT2000), *Atmos. Environ.*, 36(15/16), 2535–2544.

Bottenheim, J. W., and E. Chan (2006), A trajectory study into the origin of spring time Arctic boundary layer ozone depletion, *J. Geophys. Res.*, 111, D19301, doi:10.1029/2006JD007055.

Bottenheim, J. W., S. Netcheva, S. Morin, and S. V. Nghiem (2009), Ozone in the boundary layer air over the Arctic Ocean: measurements during the TARA transpolar drift 2006–2008, *Atmos. Chem. Phys.*, 9, 4545–4557.

Boudries, H., and J. W. Bottenheim (2000), Cl and Br atom concentrations during a surface boundary layer ozone depletion event in the Canadian High Arctic, *Geophys. Res. Lett.*, 27(4), 517–520, doi:10.1029/1999GL011025.

Curry, J. A. (1986), Interactions among turbulence, radiation, and microphysics in Arctic stratus clouds, *J. Atmos. Sci.*, 43, 90– 106.

Curry, J. A., et al. (2000), FIRE Arctic Clouds Experiment, *Bull. Am. Meteorol. Soc.*, 81, 5 – 29.

Eneroth, K., K. Holmen, T. Berg, N. Schmidbauer, and S. Solberg (2007), Springtime depletion of tropospheric ozone, gaseous elemental mercury and non-methane hydrocarbons in the European Arctic, and its relation to atmospheric transport, *Atmos. Environ.*, 41, 8511–8526.

Fan, S. M., and D. J. Jacob (1992), Surface ozone depletion in Arctic spring sustained by bromine reactions on aerosols, *Nature*, 359, 524– 552.

Finger, J. E., and P. Wendling (1990), Turbulence structure of Arctic stratus clouds derived from measurements and calculations, *J. Atmos. Sci.*, 47, 1351-1373.

Frieß, U., H. Sihler, R. Sander, D. Pöhler, S. Yilmaz, and U. Platt (2011), The Vertical Distribution of BrO and Aerosols in the Arctic: Measurements by Active and Passive DOAS, *J. Geophys. Res.*, doi:10.1029/2011JD015938, in press.

Gong, S. L., J. L. Walmsley, L. A. Barrie, and J. F. Hopper (1997), Mechanisms for surface ozone depletion and recovery during polar sunrise, *Atmos. Environ.*, *31*, 969–981.

Grannas, A. M., et al. (2007), An overview of snow photochemistry: Evidence, mechanisms and impacts, *Atmos. Chem. Phys.*, 7, 4165– 4283.

Grell, G. A., et al. (2005), Fully coupled ‘‘online’’ chemistry within the WRF model, *Atmos. Environ.*, 39, 6957–6975.

Hara, K., K. Osada, M. Yabuki, G. Hashida, T. Yamanouchi, M. Hayashi, M. Shiobara, C. Nishita, and M. Wada (2010), Haze episodes at Syowa Station, coastal Antarctica: Where did they come from?, *J. Geophys. Res.*, 115, D14205, doi:10.1029/2009JD012582.

Harrington, J. Y., and P. Q. Olsson (2001), On the potential influence of ice nuclei on surface-forced marine stratocumulus cloud dynamics, *J. Geophys. Res.*, 106, 27,473–27,484, doi:10.1029/2000JD000236.

Helmig, D., S. J. Oltmans, D. Carlson, J.-F. Lamarque, A. Jones, C. Labuschagne, K. Anlauf, and K. Hayden (2007), A review of surface ozone in the polar regions, *Atmos. Environ.*, 41, 5138–5161.

Hopper, J. F., and W. Hart (1994), Meteorological aspects of the 1992 Polar Sunrise Experiment, *J. Geophys. Res.*, 99(D12), 25,315–25,328, doi:10.1029/94JD02400.

Hopper, J.F., L.A. Barrie, A. Silis, A.J. Gallant, W. Hart, and H. Dryfhout (1998), Ozone and meteorology during the 1994 Polar Sunrise Experiment, *J. Geophys. Res.*, 103D (1), 1481–1492.

Intrieri, J. M., M. D. Shupe, T. Uttal, and B. J. McCarty (2002), An annual cycle of Arctic cloud characteristics observed by radar and lidar at SHEBA, *J. Geophys. Res.*, 107(C10), 8030, doi:10.1029/2000JC000423.

Jacobi, H.-W., L. Kaleschke, A. Richter, A. Rozanov, and J. P. Burrows (2006), Observation of a fast ozone loss in the marginal ice zone of the Arctic Ocean, *J. Geophys. Res.*, 111, D15309, doi:10.1029/2005JD006715.

Jacobi, H.-W., S. Morin, and J. W. Bottenheim (2010), Observation of widespread depletion of ozone in the springtime boundary layer of the central Arctic linked to mesoscale synoptic conditions, *J. Geophys. Res.*, 115, D17302, doi:10.1029/2010JD013940.

Klein, S., et al. (2009), Intercomparison of model simulations of mixedphase clouds observed during the ARM Mixed-Phase Arctic Cloud Experiment. Part I: Single layer cloud, *Q. J. R. Meteorol. Soc.*, 135, 979–1002.

Komurcu, M. (2011), effects of ice nuclei concentrations, ice nucleation mechanisms and ice crystal habits on the dynamics and microphysics of arctic mixed-phase clouds, Ph.D. dissertation, Penn. State Univ., University Park, August.

Leaitch, W. R., L. A. Barrie, J. W. Bottenheim, S. M. Li, P. B. Shepson, P. B. Muthuramu, and Y. Yokouchi (1994), Airborne observations related to ozone depletion at polar sunrise, *J. Geophys. Res.*, 99D, 25449–25517.

Lehrer, E., G. Honninger, and U. Platt (2004), A one dimensional model study of the mechanism of halogen liberation and vertical transport in the polar troposphere, *Atmos. Chem. Phys.*, 4, 2427–2440.

Mickle, R.E., J. W. Bottenheim, W. R. Leaitch, and W. Evans (1989), Boundary layer ozone depletion during AGASP-II, *Atmos. Environ.*, 23(11), 2443–2449.

Moeng, C.-H., and U. Schumann (1991), Composite structure of plumes in stratus-topped boundary layers, *J. Atmos. Sci.*, 48, 2280–2290.

Morrison, H., and J. O. Pinto (2006), Intercomparison of bulk cloud microphysics schemes in mesoscale simulations of springtime arctic mixed-phase stratiform clouds, *Mon. Weather Rev.*, 134, 1880– 1900.

Morrison et al. (2011), Intercomparison of cloud model simulations of Arctic mixed-phase boundary layer clouds observed during SHEBA/FIRE-ACE, *J. Adv. Model. Earth Syst.*, *3*, M06003, 23 pp., doi:10.1029/2011MS000066.

Oltmans, S. J. (1981), Surface ozone measurements in clean air, *J. Geophys. Res.*, 86(C2), 1174–1180.

Oltmans, S.J., *et al.*(1989), Seasonal surface ozone and filterable bromine relationship in the high Arctic, *Atmos. Environ.*, 23(11), 2431–2441.

Pinto, J. O. (1998), Autumnal mixed-phase cloudy boundary layers in the Arctic, *J. Atmos. Sci.*, 55, 2016– 2038.

Piot, M., and R. von Glasow (2008), The potential importance of frost flowers, recycling on snow, and open leads for ozone depletion events, *Atmos. Chem. Phys.*, 8, 2437–2467.

Rankin, A. M., E. W. Wolff, and S. Martin (2002), Frost flowers: implications for tropospheric chemistry and ice core interpretation, *J. Geophys. Res.*, 107(D23), 4683, doi:0.1029/2002JD002492.

Rasmussen, A., S. Kiilsholm, J. H. Sorensen and H. B. Mikkelsen (1997), Analysis of tropospheric ozone measurements in Greenland, *Tellus,* 49B, 510–521.

Shupe, M. D., P. Kollias, P. O. G. Persson, and G. M. McFarquhar (2008), Vertical motions in arctic mixed-phase stratiform clouds, *J. Atmos. Sci.*, 65, 1304–1322, doi:10.1175/2007JAS2479.1.

Simpson, W. R., et al. (2007), Halogens and their role in polar boundary-layer ozone depletion, *Atmos. Chem. Phys.*, 7, 4375–4418.

Solberg, S., N. Schmidtbauer, A. Semb, and F. Stordal (1996), Boundary-layer ozone depletion as seen in the Norwegian Arctic in spring, *J. Atmos. Chem.,* 23, 301–332.

Solomon, A., H. Morrison, O. Persson, M. D. Shupe, and J. W. Bao (2009), Investigation of microphysical parameterizations of snow and ice in arctic clouds during M-PACE through model-observation comparisons, *Mon. Weather Rev.*, 137, 3110–3128.

Solomon, A., M. D. Shupe, P. O. G. Persson, and H. Morrison (2011), Moisture and dynamical interactions maintaining decoupled Arctic mixed-phase stratocumulus in the presence of a humidity inversion, *Atmos. Chem. Phys. Discuss.*, 11, 13469-13524, doi:10.5194/acpd-11-13469-2011.

Strong, C., J. D. Fuentes, R. E. Davis, and J. W. Bottenheim (2002), Thermodynamic attributes of Arctic boundary layer ozone depletion, *Atmos. Environ.*, 36, 2641–2652.

Sumner, A. L., and P. B. Shepson (1999), Snowpack production of formaldehyde and its impact on the Arctic troposphere, *Nature*, 398, 230–233.

Tarasick, D. W., and J. W. Bottenheim (2002), Surface ozone depletion episodes in the Arctic and Antarctic from historical ozonesonde records, *Atmos. Chem. Phys.*, 2(3), 197–205.

Verlinde, J., et al. (2007), The Mixed-Phase Arctic Cloud Experiment, *Bull. Am. Meteorol. Soc.*, 88, 205– 221.

Wang, S., Q. Wang, R. E. Jordan, and P. O. G. Persson (2001), Interactions among longwave radiation of clouds, turbulence, and snow surface temperature in the Arctic: A model sensitivity study, *J. Geophys. Res.*, 106, 15,323–15,333, doi:10.1029/2000JD900358.

Zuidema, P., B. Baker, Y. Han, J. Intrieri, J. Key, P. Lawson, S. Matrosov, M. Shupe, R. Stone, and T. Uttal (2005), An Arctic springtime mixed-phase cloudy boundary layer observed during SHEBA, *J. Atmos. Sci.*, 62, 160–176.

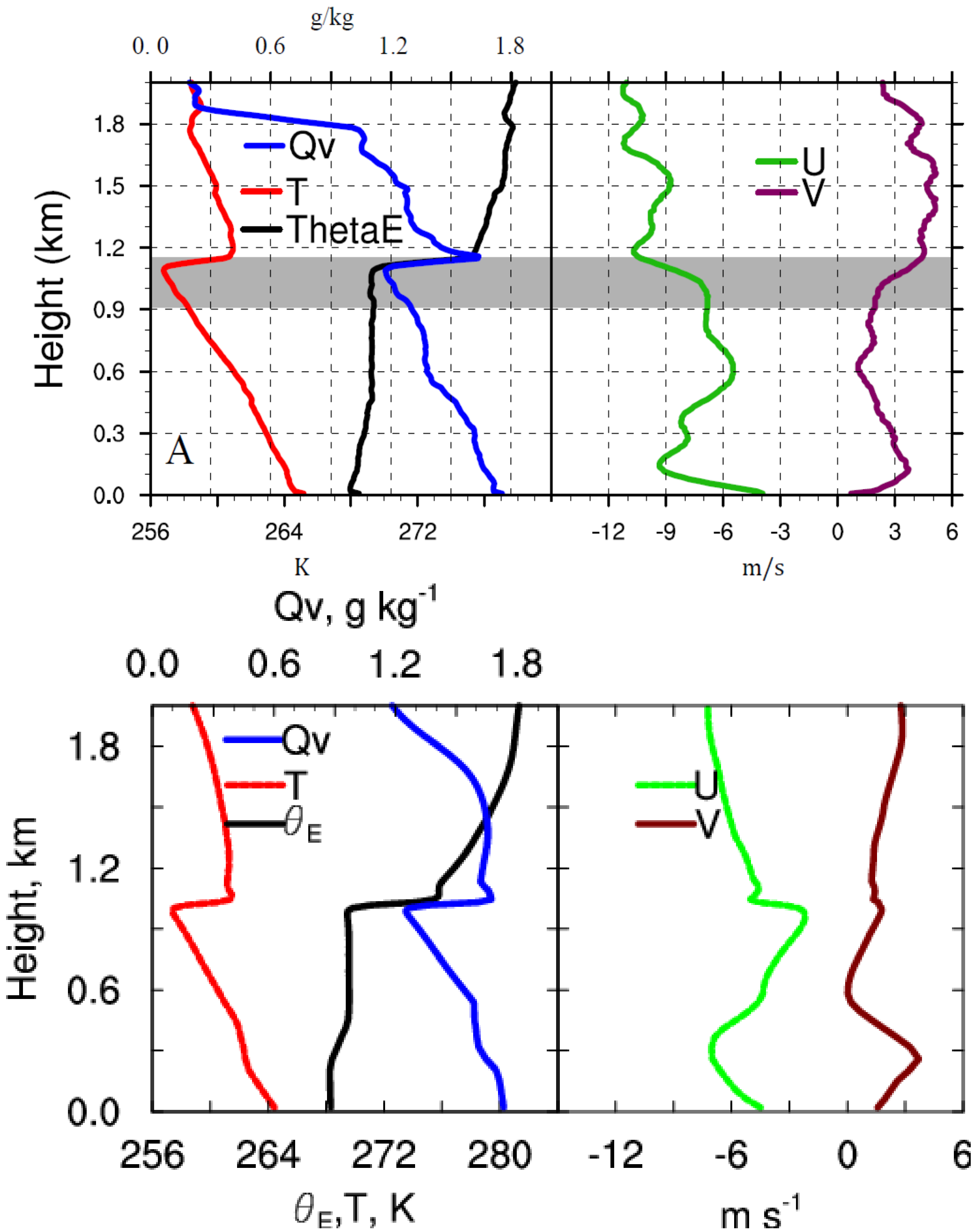

Figure 1. (Top) measured at 17.6 UTC and (bottom) simulated at 18 UTC profiles of temperature, equivalent potential temperature (θ_E), U, and V on April 8, 2008 at (71.33° N, 156.61° W). The measurement in the top panel is adapted from Solomon et al. (2011).

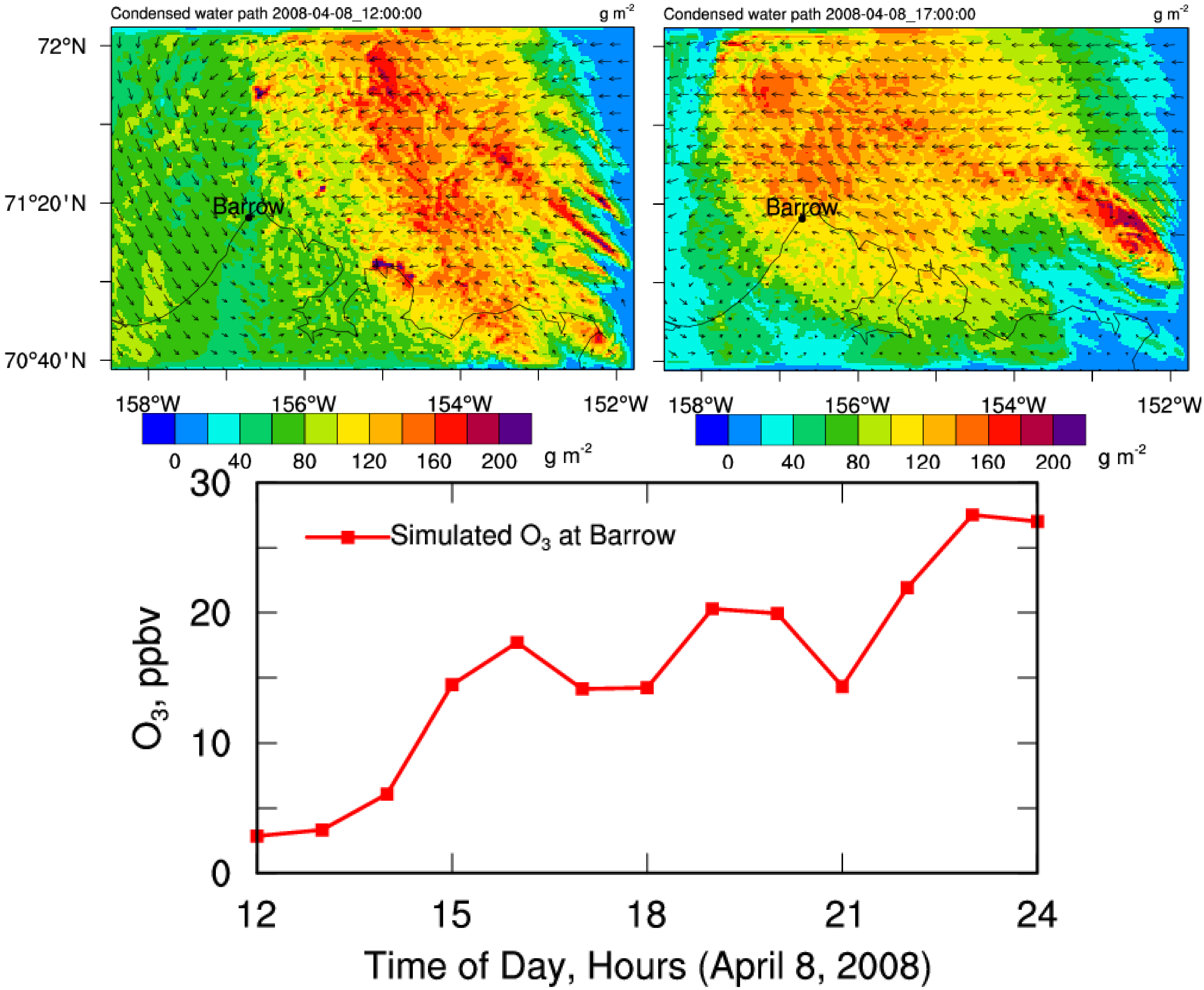

Figure 2. (Top) Column condensed water (cloud water plus cloud ice) path at 12 (before cloud passing Barrow) and 17 UTC (cloud present at Barrow) and (bottom) simulated surface O_3 at Barrow.

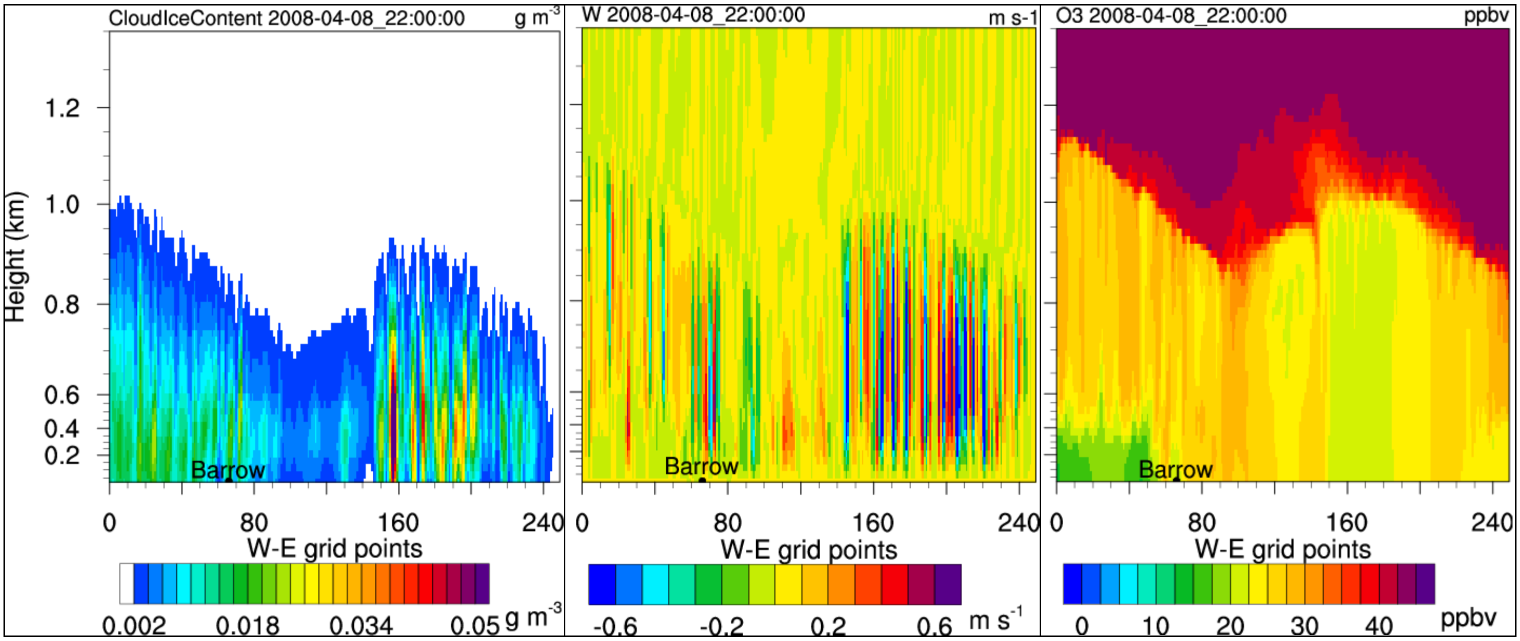

Figure 3. Simulated vertical structure of (left to right) cloud ice content, vertical velocity, and O_3 for the west-east cross section passing through Barrow, AK at 22 UTC on April 8, 2008

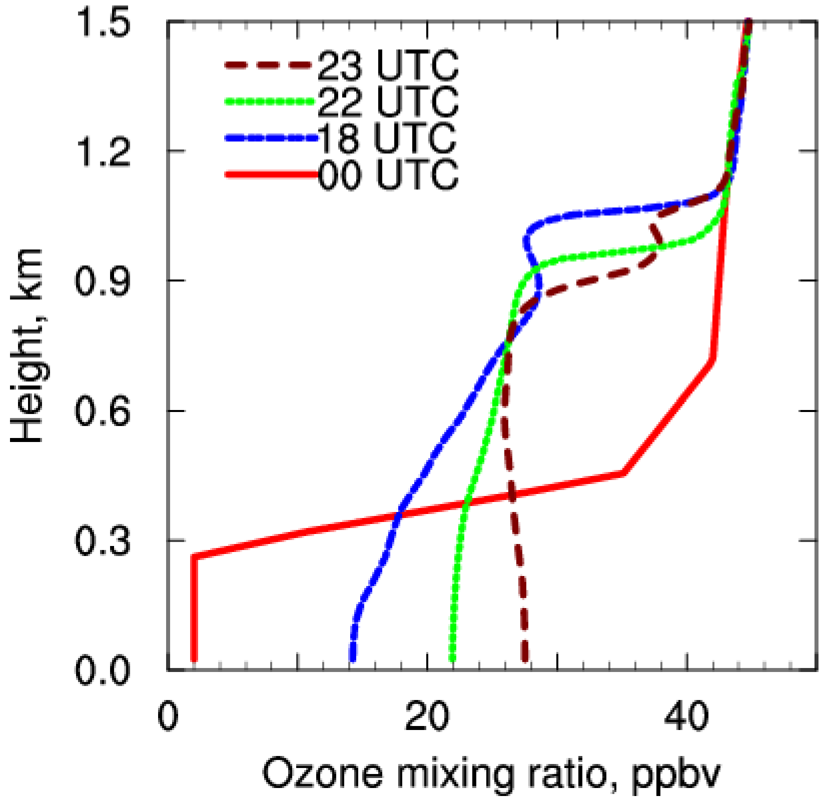

Figure 4. Initial vertical O_3 profile at 00 UTC and simulated O_3 profiles at 18, 22, and 23 UTC at Barrow, AK.